JACS
JOURNAL OF THE AMERICAN CHEMICAL SOCIETY
pubs.acs.org/JACS
Article

# Water and the Cation–$\pi$ Interaction

Yujie Zhu, Minmin Tang, Huibin Zhang, Faiz-Ur Rahman, Pablo Ballester, Julius Rebek, Jr., Christopher A. Hunter,* and Yang Yu*

Cite This: J. Am. Chem. Soc. 2021, 143, 12397–12403
Read Online
ACCESS | Metrics & More | Article Recommendations | Supporting Information

**ABSTRACT:** The cation–$\pi$ interaction and the hydrophobic effect are important intermolecular forces in chemistry and play major roles in controlling recognition in biological systems. We compared their relative contributions to the binding of molecular "dumbbell" guests in synthetic container hosts in water. The guests offered direct, intramolecular competition between trimethylammonium groups, $-N^+(CH_3)_3$, and *tert*-butyl groups, $-C(CH_3)_3$, for the internal surfaces (aromatic panels) of the containers. In contrast with previous studies, the container molecules consistently preferred binding to the uncharged *tert*-butyl groups, regardless of the presence of anionic, cationic, or zwitterionic groups on the container peripheries. This preference is determined by solvation of the polar trimethylammonium group in water, which outcompetes the attraction between the positive charge and the $\pi$-surfaces in the container. The synthetic container complexes provide a direct measure of the relative strengths of cation–$\pi$ interactions and desolvation in water. Interactions with the uncharged *tert*-butyl group are more than 12 kJ mol$^{-1}$ more favorable than the cation–$\pi$ interactions with the trimethylammonium group in these cavitand complexes.

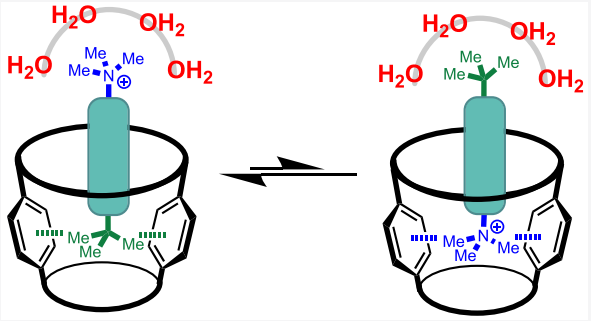


## INTRODUCTION

The cation–$\pi$ interaction and the desolvation of hydrophobic groups are recognized as important forces for complex formation in water and often control the recognition properties of biological systems. Cation–$\pi$ interactions were invoked in the binding of organic and inorganic cations by synthetic receptors, in supramolecular catalysis, and in X-ray crystal structures of small molecules and supramolecular complexes.[1−7] Hydrophobic interactions are ubiquitous in biology and are involved whenever nonpolar residues (i.e., C–H bonds) appear in small molecules or their macromolecular targets. In addition, cation–$\pi$ interactions are implicated in the mechanism of action of ion channels and in the recognition of ammonium groups, which are found in a range of important biological signaling molecules, such as acetyl choline.[8−13] One may well ask which is the stronger driving force, the cation–$\pi$ or the (often harder to evaluate) hydrophobic effect, in given situations, and we offer some comparisons here.

An attractive experiment is to compare the free energy gain for a complex involving an interaction between an aromatic ring and a trimethylammonium group with that of an analogous complex in which the latter group is replaced by a *t*-butyl counterpart (Figure 1). The groups are isosteric, so the difference between the two equilibria shown in Figure 1 should provide a direct measure of the contribution of the positive charge to the overall stability of the complex provided by the cation–$\pi$ interaction ($\Delta\Delta G = \Delta G_2 - \Delta G_1$).

At first glance, the less polarized CH bonds of the *t*-butyl predict that CH–$\pi$ interactions will be weaker than the cation–$\pi$ interaction, and this is borne out in nonpolar media.[14−21] However, the formation of an intermolecular complex in solution is a competition that also involves the solvent–solute and solvent–solvent interactions. In a polar solvent, more favorable solvation of the polar cation predicts that the cation–$\pi$ interaction will be weaker than the interaction with the *t*-butyl group (Figure 1). In water, the situation is further complicated by the hydrophobic effect, which drives the escape of nonpolar surfaces from water. Here we describe experiments designed to distinguish between the effects of the positive charge and desolvation for cation–$\pi$ interactions in water.

The experiment shown in Figure 1 has been carried out for a number of biomolecular complexes.[22,23] Many of these experiments suggest that in water the complex involving the ammonium•aromatic interaction is more stable than that featuring the *t*-butyl•aromatic interaction, but this is not true for all systems. A particularly interesting example was reported by Diederich, who carried out the comparison for two closely

Received: June 23, 2021
Published: July 30, 2021

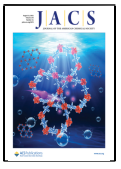







https://doi.org/10.1021/jacs.1c06510
J. Am. Chem. Soc. 2021, 143, 12397–12403

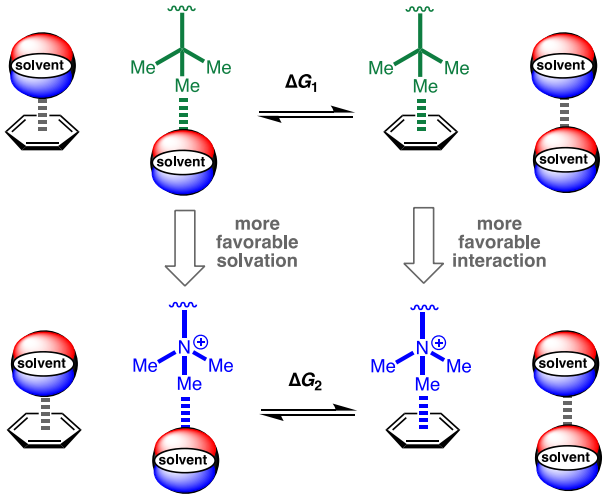


**Figure 1.** Comparison of a *t*-butyl•aromatic interaction with a trimethylammonium•aromatic interaction quantifies the contribution of the positive charge to the cation–$\pi$ interaction in solution ($\Delta\Delta G = \Delta G_2 - \Delta G_1$). The relative strengths of the solvent interactions highlighted play an important role in determining which complex is more stable because compared with the nonpolar *t*-butyl group, the polar trimethylammonium makes more favorable interactions with both the solvent and the aromatic $\pi$-electron density.

related enzymes, thrombin and Factor Xa, where a trimethylammonium•tryptophan contact was identified by X-ray crystallography.[24] For Factor Xa, $\Delta\Delta G$ was −12 kJ mol$^{-1}$, suggesting that the cation–$\pi$ interaction stabilizes the complex, but for thrombin, $\Delta\Delta G$ was +10 kJ mol$^{-1}$, indicating that the positive charge has a destabilizing effect on binding. A similar experiment on folding of a peptide hairpin concluded that the trimethylammonium group binds to an aromatic surface better than a *t*-butyl group.[25] One potential problem with the experiments on biomolecules of such complexity is that there are many charged residues that could play a role in the observed selectivity. Electrostatic interactions between charged groups can be significant over long distances, and these effects could compromise the experimental results, where the overall charges on the *t*-butyl and ammonium groups are different. Synthetic supramolecular systems provide an opportunity to investigate the fundamental properties of noncovalent interactions in a stripped-down context that removes all of the complexity associated with the conformational dynamics and functional group diversity found in biomolecules. Here we use the complexation of molecular dumbbells by synthetic receptors to investigate the nature of the cation–$\pi$ interaction in water.

## RESULTS

Cavitands are synthetic container compounds (hosts) that bind guests in aqueous ($D_2O$) solution. The deep cavitands have a highly preorganized nonpolar binding pocket, lined with the $\pi$-faces of eight electron-rich aromatic rings. The aromatic panels create a magnetic anisotropy for guest nuclei held inside the cavity, which results in upfield shifts of the $^1$H NMR resonances of bound guests. The upfield shifts correlate with the depth in the cavity.[26−29] Earlier studies in related cavitands showed that both *t*-butyl and trimethylammonium groups are accommodated in the cavity and occupy the same position, at the bottom of the binding pocket.[30] For example, a *t*-butyl group bound inside a cavitand typically gives rise to a $^1$H NMR signal at −3.1 ppm ($\Delta\delta$ −4.4 ppm relative to the free guest), and a trimethylammonium group gives a signal at −1.2 ppm ($\Delta\delta$ −4.9 ppm). These systems therefore provide an ideal platform for investigating the cation–$\pi$ interaction using the experiment illustrated in Figure 1.

Figure 2 shows the structures of the eight different cavitands used in this study. These receptors all have the same aromatic

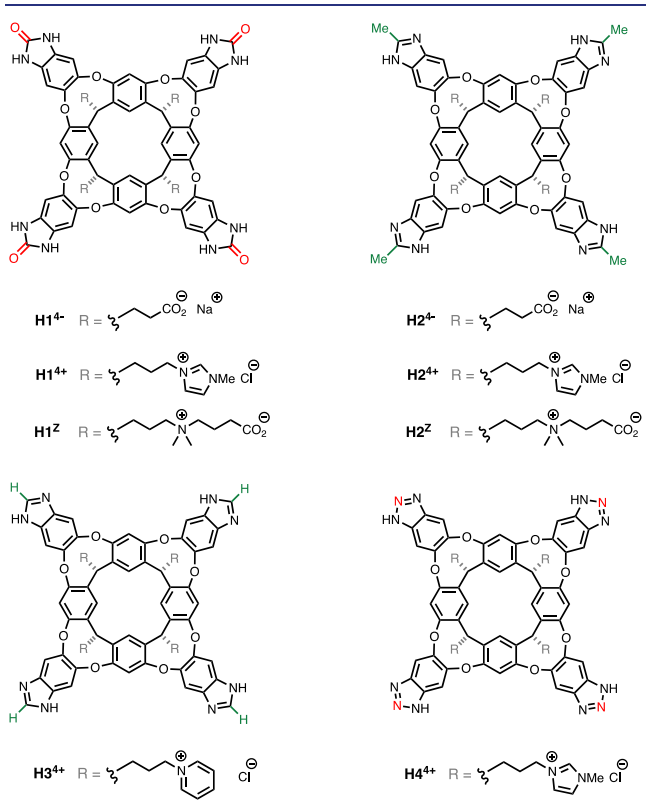


**Figure 2.** Eight cavitand hosts which differ only in the polarity of the functional groups presented on the upper rim of the binding pocket (red and green) and the charges on the water solubilizing groups that extend from the base of the cavity (gray).

binding pocket but differ in the polarity of the functional groups that line the entrance to the binding site and the charges on the peripheral water solubilizing groups. For the tetraurea cavitand (**H1**) and the tetramethylbenzimidazole cavitand (**H2**), three versions equipped with different solubilizing groups were prepared: anionic, cationic, or zwitterionic. These ionic groups are remote from the binding pocket, on the outside side of the aromatic walls, and provide an opportunity to study the effects of long-range electrostatic interactions on guest binding.

We devised a competition experiment using the dumbbell guests shown in Figure 3, which have a trimethylammonium group at one end and a *t*-butyl group at the other. Interaction of the dumbbell guests with the cavitand hosts allows measurement of the contribution of the positive charge to the cation–$\pi$ interaction in water directly from the equilibrium constant between the two binding geometries of the complex shown in Figure 4. The linkers connecting the two head groups are symmetric in all cases, so any interactions between the linker and the walls of the cavitand will not affect the position of equilibrium. The equilibrium constant measured in this experiment can be used to obtain a free energy difference ($\Delta G = -RT \ln K$) which is equivalent to $\Delta G_2 - \Delta G_1$ in Figure 1.


https://doi.org/10.1021/jacs.1c06510
J. Am. Chem. Soc. 2021, 143, 12397−12403

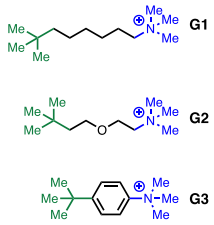


**Figure 3.** Three symmetric dumbbell guests which differ in the length of the spacer separating the charged (blue) and neutral (green) head groups.

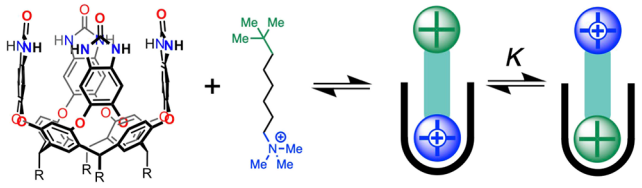


**Figure 4.** Schematic representation of the two isomeric complexes that can be formed between a cavitand host and a dumbbell guest. *K* is defined as the equilibrium constant in favor of the *t*-butyl-in isomer.

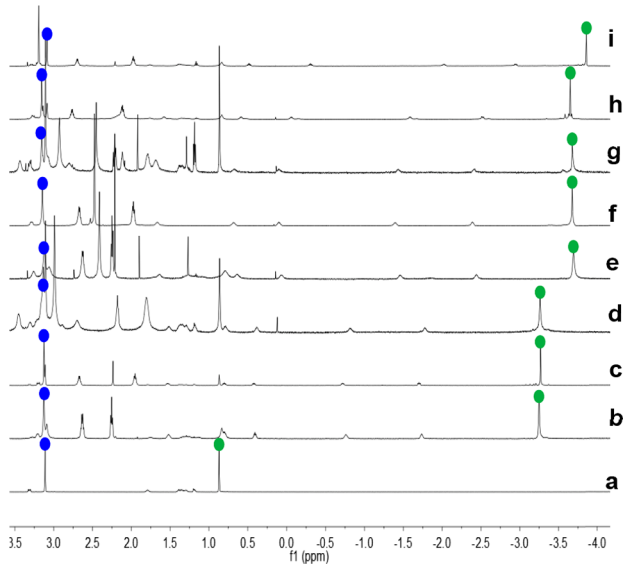


**Figure 5.** Partial $^1$H NMR spectra of 1 mM solutions of **G1** before the addition of host (a) and in the presence of one equivalent of $\mathbf{H1}^{4-}$, $\mathbf{H1}^{4+}$, $\mathbf{H1}^{Z}$, $\mathbf{H2}^{4-}$, $\mathbf{H2}^{4+}$, $\mathbf{H2}^{Z}$, $\mathbf{H3}^{4+}$, or $\mathbf{H4}^{4+}$ (b–i, respectively). Blue dots indicate the signals due to the protons of the trimethylammonium group, and green dots indicate the signals due to the protons of the *t*-butyl group.

However, in this case the difference between the *t*-butyl and trimethylammonium complexes is an isomerization, so the overall charges of the two complexes are identical, and any effects on the value of $\Delta G$ are removed. The three guests were prepared as the iodide salts, and in principle, ion-pairing interactions between the trimethylammonium head group and the iodide counterion could bias the equilibrium in Figure 4 toward the *t*-butyl-in isomer. However, the association constant for formation of an ion pair between a trimethylammonium group and iodide in aqueous solution is 2–5 $M^{-1}$.[31] The experiments described below were all carried out at guest concentrations of 1 mM, so the counterion is fully dissociated (>99%) in all cases and does not influence the experiment.

Interaction of the three dumbbell guests (**G1**, **G2**, and **G3**) with the eight cavitands ($\mathbf{H1}^{4-}$, $\mathbf{H1}^{4+}$, $\mathbf{H1}^{Z}$, $\mathbf{H2}^{4-}$, $\mathbf{H2}^{4+}$, $\mathbf{H2}^{Z}$, $\mathbf{H3}^{4+}$, and $\mathbf{H4}^{4+}$) was investigated by NMR spectroscopy. All 24 systems formed 1:1 complexes with slow exchange between the free and bound states on the $^1$H NMR time scale (see the Supporting Information for the full spectra). The guest with the longest linker **G1** showed remarkably consistent behavior. Figure 5 shows the upfield region of the $^1$H NMR spectra of the eight **G1** complexes, and the spectrum of the free guest is shown in Figure 5a. The signal due to the trimethylammonium group in the complex (blue dot) has a very similar chemical shift to the free guest, whereas the signal due to the bound *t*-butyl group (green dot) appears at around −3 ppm, an upfield shift of 4 ppm relative to the free guest. All of the $^1$H NMR spectra of the complexes in Figure 5 have two additional signals in the upfield region: −0.8 and −1.8 ppm in Figures 5b–5d, −1.5 and −2.5 ppm in Figures 5e–5g, and at slightly lower chemical shifts in Figures 5h and 5i. These signals are due to the methylene protons $\alpha$ and $\beta$ to the *t*-butyl group and are not due to the other isomer of the complex which has the trimethylammonium group inside the binding pocket. The NMR spectra in Figure 5 indicate that in all eight complexes—regardless of the charge on the host or the polarity of the functional groups that line the entrance to the binding pocket—the *t*-butyl end of the guest is preferentially bound in the cavitand pocket, and the trimethylammonium group is exposed to water.

The behavior of the other two dumbbell guests **G2** and **G3** was more complicated. With cavitands $\mathbf{H1}^{4-}$, $\mathbf{H1}^{4+}$, $\mathbf{H1}^{Z}$, $\mathbf{H3}^{4+}$, and $\mathbf{H4}^{4+}$, a single set of bound guest signals was observed for all 10 complexes. The $^1$H NMR spectra of the complexes resemble those shown for **G1** in Figure 5 (see the Supporting Information). The signal due to the trimethylammonium group appears at the same chemical shift as the free guest, and the signal due to the *t*-butyl group shows an upfield shift of 4 ppm; i.e., the *t*-butyl end of the guest is preferentially bound in the cavitand pocket. In contrast, there are two sets of bound guest signals in slow exchange in the $^1$H NMR spectra of the complexes formed with the tetramethylbenzimidazole cavitands $\mathbf{H2}^{4-}$, $\mathbf{H2}^{4+}$, and $\mathbf{H2}^{Z}$. Figure 6 and Figure 7 show the upfield region of the $^1$H NMR spectra of these six complexes. For one set of bound guest signals, the signal due to the trimethylammonium group (single blue dot) appears at the same chemical shift as the free guest, and the signal due to the *t*-butyl group (single green dot) appears at around −3 ppm, an upfield shift of 4 ppm relative to the free guest. For the other set of bound guest signals, the signal due to the *t*-butyl group appears at the same chemical shift as the free guest (double green dot), and the signal due to the trimethylammonium group (double blue dot) appears at around −1 ppm, an upfield shift of 4 ppm relative to the free guest.

These results show that both of the isomeric complexes shown in Figure 4 are populated. Integration of the two sets of bound guest signals in the $^1$H NMR spectra in Figures 6 and 7 allowed direction measurement of the equilibrium constant *K* defined in Figure 4 and hence determination of the free energy difference $\Delta G$. The results are summarized in Table 1. For the positively charged receptor $\mathbf{H2}^{4+}$, there is a 3–4 kJ $mol^{-1}$ driving force in favor of the *t*-butyl end of the guest binding in the cavitand pocket. For the negatively charged receptor $\mathbf{H2}^{4-}$, there is a 3–4 kJ $mol^{-1}$ driving force in favor of the


https://doi.org/10.1021/jacs.1c06510
J. Am. Chem. Soc. 2021, 143, 12397–12403

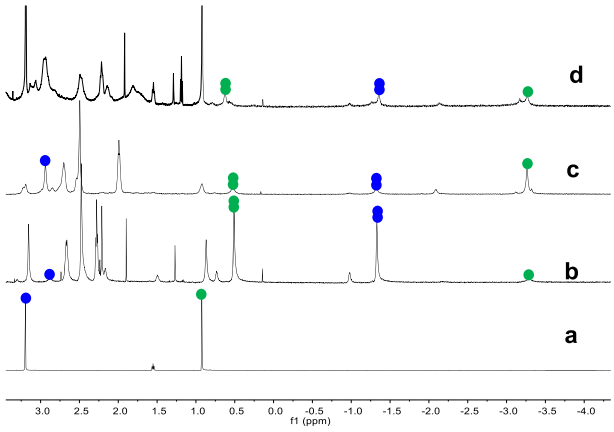


**Figure 6.** Partial $^1$H NMR spectra of 1 mM solutions of **G2** before the addition of host (a) and in the presence of one equivalent of $\mathbf{H2}^{4-}$, $\mathbf{H2}^{4+}$, or $\mathbf{H2}^{Z}$ (b–d, respectively). Blue dots indicate the signals due to the protons of the trimethylammonium group, and green dots indicate the signals due to the protons of the *t*-butyl group. In each case, there are two sets of bound guest signals, one indicated by single dots and the other indicated by double dots.

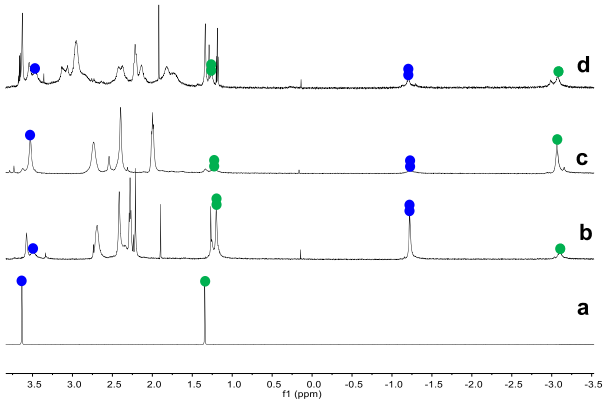


**Figure 7.** Partial $^1$H NMR spectra of 1 mM solutions of **G3** before the addition of host (a) and in the presence of one equivalent of $\mathbf{H2}^{4-}$, $\mathbf{H2}^{4+}$, or $\mathbf{H2}^{Z}$ (b–d, respectively). Blue dots indicate the signals due to the protons of the trimethylammonium group, and green dots indicate the signals due to the protons of the *t*-butyl group. In each case, there are two sets of bound guest signals, one indicated by single dots and the other indicated by double dots.

**Table 1. Free Energy Difference ($\Delta G$ in kJ mol$^{-1}$) Measured in Water for the Equilibrium between the Two Isomeric Complexes in Figure 4**[a]

| | guest | | |
|---|---|---|---|
| cavitand | G1 | G2 | G3 |
| $\mathbf{H2}^{4-}$ | <−8 | 4.3 | 2.7 |
| $\mathbf{H2}^{Z}$ | <−8 | −0.2 | −1.0 |
| $\mathbf{H2}^{4+}$ | <−8 | −3.4 | −4.0 |

[a]A negative value of $\Delta G$ means that the *t*-butyl in the isomer is favored relative to the cation–$\pi$ isomer.

trimethylammonium end of the guest binding in the cavitand pocket. For zwitterionic receptor $\mathbf{H2}^{Z}$, the free energy difference is close to zero. The location of the charged solubilizing groups in these cavitands means that they are closer to the trimethylammonium group when it is bound in the cavitand pocket than in the other isomer. The results in Table 1 therefore appear to be the result of long-range electrostatic interactions through the base of the cavitand between the charged solubilizing groups and the charge on the guest: negatively charged cavitands favor the cation–$\pi$ isomer, and positively charged cavitands destabilize the cation–$\pi$ isomer. It would be interesting to investigate the influence of counterion and ionic strength on these measurements, but unfortunately the cavitands have limited solubility in the presence of salts.

Molecular modeling provides further insight into the difference in behavior observed for these complexes. Figure 8 shows three-dimensional structures of the **H1** and **H2** complexes optimized using DFT and a water solvation model (see the Supporting Information for details). For all of the complexes with dumbbell guest **G1**, one of the head groups is located inside the cavitand binding pocket, and the other is directed outward into the solvent (Figures 8a and 8d). In this case, the linker is sufficiently long that the only contacts the functional groups on the upper rim of the cavitand can make with the guest are via the methylene groups of the linker rather than either of the head groups. These structures explain why **G1** gives the same result for all cavitands.

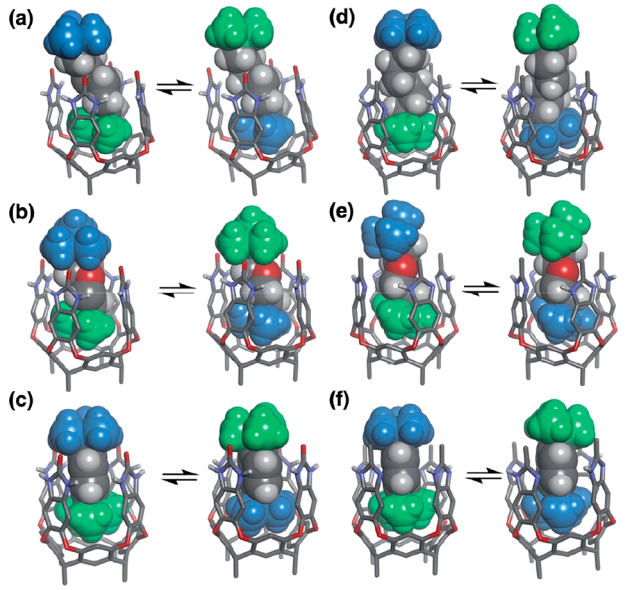


**Figure 8.** Energy-minimized structures of (a) **H1•G1**, (b) **H1•G2**, (c) **H1•G3**, (d) **H2•G1**, (e) **H2•G2**, and (f) **H2•G3**. The cavitand solubilizing groups were replaced by methyl groups, and explicit water molecules that form H-bonded bridges between the urea and imidazole nitrogens are not shown for clarity. Structures were optimized using DFT bp86-def2tzvp with empirical dispersion correction bj-D3 and COSMO water solvation.

When the length of the linker is shorter (as in **G2** shown in Figures 8b and 8e and **G3** shown in Figures 8c and 8f), the methyl groups of the external head group of the guest make close contacts with the carbonyl oxygen atoms of the tetraurea cavitands in the **H1** complexes and with the methyl groups of the tetramethylbenzimidazole cavitands in the **H2** complexes. These additional interactions between the cavitand and the head groups perturb the equilibrium between the two isomeric complexes. Figure 9 illustrates the outcome schematically. The polar trimethylammonium head group can make attractive interactions with the rim of the tetraurea cavitands **H1**, which increases the stability of this isomer. The nonpolar *t*-butyl head


https://doi.org/10.1021/jacs.1c06510
J. Am. Chem. Soc. 2021, 143, 12397–12403

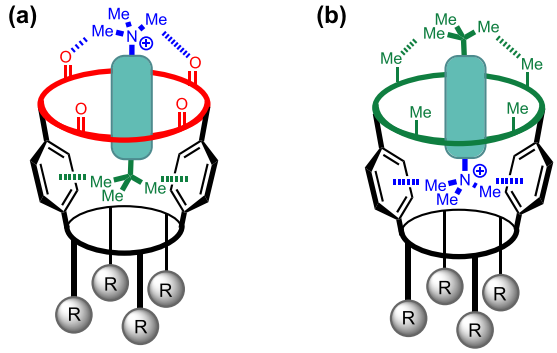


**Figure 9.** For dumbbell guests with short linkers, the external head group comes into contact with the upper rim of the cavitand hosts. (a) The polar urea groups in **H1** (red) make attractive interactions with the cationic head group. (b) The hydrophobic methyl groups in **H2** (green) make attractive interactions with the *t*-butyl head group.

group can make hydrophobic interactions with the rim of the tetramethylbenzimidazole cavitands **H2**, which favors the cation−$\pi$ isomer. These interactions between the head groups and the upper rim of the cavitands are the reason why the cation−$\pi$ isomer is only observed for the complexes of **H2** with the shorter dumbbell guests.

## DISCUSSION

Although experimental measurements show that the cation−$\pi$ interaction is attractive in the gas phase and in nonpolar organic solvents,[32−35] the situation in water is more complicated. Molecular recognition in solution involves competition with solvent interactions, and the thermodynamics of desolvation are particularly significant in water.[36−40] The role of solvation in the interaction between quaternary ammonium groups and aromatic rings in biomolecular systems is not straightforward because although both binding partners have a hydrocarbon surface, the ammonium group is a cation that should also interact well with water. The direct competition experiment staged here using molecular dumbbell **G1** provides a direct measure of the effect of the positive charge on a quaternary ammonium group on the relative strengths of the interactions made with the water molecules in the solvation shell and the interactions made with the $\pi$-electron density of the aromatic rings of a receptor (Figure 10). The only difference between the two complexes shown in Figure 10 is the location of the positive charge, which can either reside on the group solvated by water or the group surrounded by $\pi$-electrons. Any bias due to ion pairing between the cationic head group and the iodide counterion can be ruled out because the experiments were all carried out at concentrations where the population of the ion pair is less than 1%.[31] Every one of the eight different **G1** complexes described here shows an overwhelming preference for the cation to be solvated by water in preference to cation−$\pi$ interactions in the cavitand pocket.

When the shorter dumbbells **G2** and **G3** bind to the cavitands, the external head group of the guest comes into close proximity with the functional groups that line the entrance to the binding pocket (Figure 9). Hydrophobic interactions between methyl groups on the upper rim of the **H2** cavitand and the *t*-butyl head group of **G2** and **G3** lead to sufficient stabilization of the cation−$\pi$ isomer that it is possible to quantify the equilibrium constant for the two isomeric

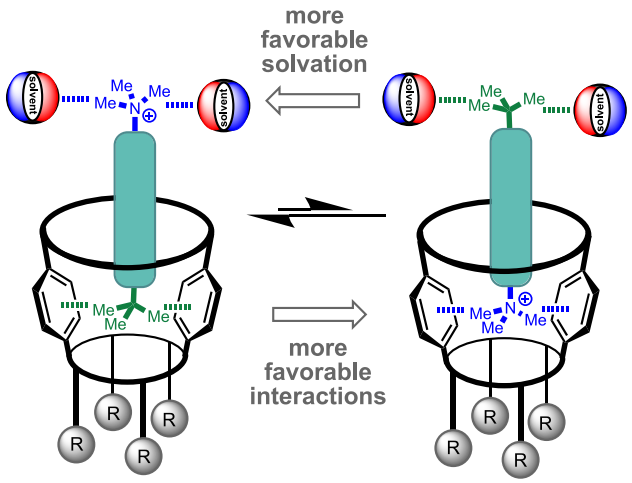


**Figure 10.** Dumbbell guest **G1** measures the difference between interactions made with the solvation shell and interactions made with the $\pi$-faces of the cavitand. The presence of the positive charge on the trimethylammonium group increases the polarity compared with the isosteric *t*-butyl group, which increases the strength of both types of interaction. In water, the equilibrium lies overwhelmingly in favor of cation solvation over cation−$\pi$ interactions. The locations of the charged solubilizing groups on the cavitands are indicated by R.

complexes. These experiments reveal the role played by long-range electrostatic interactions in water. To ensure that the remote charged groups used to solubilize the cavitands did not perturb the competition experiments, the behavior of positive, zwitterionic, and negative solubilizing groups was compared (**H2**$^{4-}$, **H2**$^{4+}$, and **H2**$^{Z}$). Even though these charges are on the outside of the cavitand and a distance from the binding pocket, electrostatic interactions with the positive charge on the trimethylammonium end of the dumbbell are sufficient to switch the preferred guest orientation from the cation−$\pi$ isomer in the negatively charged cavitand to the other isomer in the positively charged cavitand. In the complexes described here, the peripheral charged groups are well-solvated and likely to be screened by counterions. In a protein, the effects of long-range electrostatic interactions could be large if there are unscreened charged groups buried in a region of low effective dielectric constant. For example, the electrostatic interaction between two charged residues that form a salt bridge in the hydrophobic interior of a protein stabilize the folded state by about 14 kJ mol$^{-1}$.[41]

The overwhelming preference for the *t*-butyl group of **G1** to occupy the binding pocket for all of cavitands means that it is not possible to determine the free energy difference between the two different head group interactions. However, it is possible to place a lower limit on the magnitude of the effect. We have been able to measure populations down to 4% with this experiment, which places an upper limit of −8 kJ mol$^{-1}$ on the value of $\Delta G$ for each of the **G1** complexes (Table 1). Two of the **G1** complexes involve negatively charged cavitands, and the experiments on **G2** and **G3** indicate that the cation−$\pi$ isomer is favored by long-range electrostatic interactions in these systems. The zwitterionic complex **H2**$^{Z}$•**G2** is almost perfectly balanced between the two isomeric complexes, which implies that the **H2**$^{4-}$•**G2** complex can be used to estimate the electrostatic contribution due to attractive interactions between the cationic head group and the negatively solubilizing groups in the cation−$\pi$ isomer as 4 kJ mol$^{-1}$. Combining these measurements indicates that hydrophobic


https://doi.org/10.1021/jacs.1c06510
J. Am. Chem. Soc. 2021, 143, 12397−12403

interactions with the *t*-butyl group are at least 12 kJ $mol^{-1}$ more favorable than cation−$\pi$ interactions in this system.

## CONCLUSIONS

The conclusion from previous studies was that the presence of the positive charge stabilizes the cation−$\pi$ interaction in water through attractive electrostatic interactions with the $\pi$-electron density. However, the H-bond donor parameter measured for tetraalkyl ammonium cations is the almost the same as the value for water ($\alpha$ = 2.7−2.8), so the presence of the positive charge should also stabilize the interaction between the trimethylammonium cation and the solvent. Given that the lone pair of a water molecule is significantly more polar than the $\pi$-electron density of an aromatic ring, it seems likely that the presence of the positive charge would stabilize the solvated state to a greater extent. In other words, the expectation based on an electrostatic argument is that the positive charge should destabilize the cation−$\pi$ in water. The usual suspects, entropy, dispersion, and polarization, have been invoked to deal with this inconvenient truth. However, the experiments described here show that the hydrophobic effect makes the inclusion of a nonpolar *t*-butyl group in an aromatic cavity much more favorable than the inclusion of a trimethylammonium group, which makes multiple cation−$\pi$ interactions. We also show that the relative binding affinities of aromatic rings for positively charged and neutral groups are modulated by long-range electrostatic interactions with remote charges. These long-range electrostatic interactions represent a major complication for analysis of the cation−$\pi$ interaction in biomolecular systems, where there are multiple charged residues in relatively close proximity. Inspection of the original Dougherty receptor, which stimulated much of the excitement about the importance of cation−$\pi$ interactions in water, reveals that this receptor is a tetra-anion.[42]

There are important implications for biomolecular recognition processes. The experiments reported here show that the optimum substrate for binding into a cavity lined with $\pi$-faces of aromatic rings, sometimes called a $\pi$-box, is a neutral hydrocarbon rather than a quaternary ammonium cation. The more favorable aqueous solvation associated with the presence of the positive charge in the cation outcompetes any gain from cation−$\pi$ interactions made in the complex because water is more polar than the $\pi$-system. Although quaternary ammonium ions will form complexes with simple $\pi$-boxes, such as the cavitands described here, additional interactions would be required to achieve selectivity with respect to the binding of isosteric hydrophobic groups in water. The experiments reported here suggest that in biomolecular systems those additional interactions could be provided by electrostatic interactions with negatively charged functional groups remote from the binding pocket, especially if the interactions can be amplified by transmission through a low dielectric medium such as the interior of a protein. Although it is tempting to interpret binding in terms of the cation−$\pi$ interaction when a cation and an aromatic ring are observed to make a close contact in a complex, in water the major driving force is not the interaction between the positive charge and the $\pi$-electron density. Instead, desolvation and ionic interactions with remote charges are dominant.

## ASSOCIATED CONTENT

### Supporting Information

The Supporting Information is available free of charge at https://pubs.acs.org/doi/10.1021/jacs.1c06510.

Materials and methods; general experimental and synthetic procedures; $^1$H NMR and MS spectra of hosts and guests; $^1$H NMR spectra and relative $\Delta\delta$ calculation of the complexes (PDF)

## AUTHOR INFORMATION


### Corresponding Authors

**Christopher A. Hunter** − *Yusef Hamied Department of Chemistry, University of Cambridge, Cambridge CB2 1EW, United Kingdom;* orcid.org/0000-0002-5182-1859; Email: herchelsmith.orgchem@ch.cam.ac.uk

**Yang Yu** − *Center for Supramolecular Chemistry & Catalysis and Department of Chemistry, College of Science, Shanghai University, Shanghai 200444, China;* orcid.org/0000-0001-5698-3534; Email: yangyu2017@shu.edu.cn

### Authors

**Yujie Zhu** − *Center for Supramolecular Chemistry & Catalysis and Department of Chemistry, College of Science, Shanghai University, Shanghai 200444, China*

**Minmin Tang** − *Center for Supramolecular Chemistry & Catalysis and Department of Chemistry, College of Science, Shanghai University, Shanghai 200444, China*

**Huibin Zhang** − *Center for Supramolecular Chemistry & Catalysis and Department of Chemistry, College of Science, Shanghai University, Shanghai 200444, China*

**Faiz-Ur Rahman** − *Center for Supramolecular Chemistry & Catalysis and Department of Chemistry, College of Science, Shanghai University, Shanghai 200444, China;* orcid.org/0000-0002-4006-8881

**Pablo Ballester** − *Institute of Chemical Research of Catalonia (ICIQ), 43007 Tarragona, Spain; Catalan Institution for Research and Advanced Studies (ICREA), 08010 Barcelona, Spain;* orcid.org/0000-0001-8377-6610

**Julius Rebek, Jr.** − *Skaggs Institute for Chemical Biology and Department of Chemistry, The Scripps Research Institute, La Jolla, California 92037, United States;* orcid.org/0000-0002-2768-0945

Complete contact information is available at: https://pubs.acs.org/10.1021/jacs.1c06510


### Notes

The authors declare no competing financial interest.

## ACKNOWLEDGMENTS

We thank the National Natural Science Foundation of China (Grant No. 21801164 and No.22071144) and Shanghai University (N.13-0101-17-202) for financial support. Y.Y. thanks the Program for Professor of Special Appointment (Dongfang Scholarship) of the Shanghai Education Committee. We thank Y. H. Song for NMR spectroscopic assistance and G. F. Tang for MS spectroscopic assistance.

## REFERENCES

(1) Murayama, K.; Aoki, K. Molecular recognition involving multiple cation−$\pi$ interactions: the inclusion of the acetylcholine trimethylammonium moiety in resorcin[4]arene. *Chem. Commun.* **1997**, No. 1, 119−120.

(2) Dougherty, D. A. The Cation-$\pi$ Interaction. *Acc. Chem. Res.* **2013**, *46*, 885−893.
(3) Ma, J. C.; Dougherty, D. A. The Cation−$\pi$ Interaction. *Chem. Rev.* **1997**, *97*, 1303−1324.
(4) Jordan, J. H.; Gibb, B. C. Molecular containers assembled through the hydrophobic effect. *Chem. Soc. Rev.* **2015**, *44*, 547−85.
(5) Escobar, L.; Ballester, P. Quantification of the hydrophobic effect using water-soluble super aryl-extended calix[4]pyrroles. *Org. Chem. Front.* **2019**, *6*, 1738−1748.
(6) Biros, S. M.; Ullrich, E. C.; Hof, F.; Trembleau, L.; Rebek, J. Ki netically Stable Complexes in Water: The Role of Hydration and Hydrophobicity. *J. Am. Chem. Soc.* **2004**, *126*, 2870−2876.
(7) Murray, J.; Kim, K.; Ogoshi, T.; Yao, W.; Gibb, B. C. The aqueous supramolecular chemistry of cucurbit[n]urils, pillar[n]arenes and deep-cavity cavitands. *Chem. Soc. Rev.* **2017**, *46*, 2479−2496.
(8) Spath, A.; Konig, B. Molecular recognition of organic ammonium ions in solution using synthetic receptors. *Beilstein J. Org. Chem.* **2010**, *6*, 32..
(9) Mahadevi, A. S.; Sastry, G. N. Cation-$\pi$ interaction: its role and relevance in chemistry, biology, and material science. *Chem. Rev.* **2013**, *113*, 2100−2138.
(10) Kumar, K.; Woo, S. M.; Siu, T.; Cortopassi, W. A.; Duarte, F.; Paton, R. S. Cation-$\pi$ interactions in protein-ligand binding: theory and data-mining reveal different roles for lysine and arginine. *Chem. Sci.* **2018**, *9*, 2655−2665.
(11) Hong, S.; Wang, Y.; Park, S. Y.; Lee, H. Progressive fuzzy cation−$\pi$ assembly of biological catecholamines. *Sci. Adv.* **2018**, *4*, 1−10.
(12) Torrice, M. M.; Bower, K. S.; Lester, H. A.; Dougherty, D. A. Probing the role of the cation−$\pi$ interaction in the binding sites of GPCRs using unnatural amino acids. *Proc. Natl. Acad. Sci. U. S. A.* **2009**, *106*, 11919−11924.
(13) Gebbie, M. A.; Wei, W.; Schrader, A. M.; Cristiani, T. R.; Dobbs, H. A.; Idso, M.; Chmelka, B. F.; Waite, J. H.; Israelachvili, J. N. Tuning underwater adhesion with cation−$\pi$ interactions. *Nat. Chem.* **2017**, *9*, 473−479.
(14) Yumura, T.; Ishikura, M.; Urita, K. Why Pore Width of Nanoporous Carbon Materials Determines the Preferred Solvated States of Alkaline Cations: A Density Functional Theory Calculation Study. *J. Phys. Chem. C* **2019**, *123*, 21457−21466.
(15) Yamada, S. Cation-$\pi$ Interactions in Organic Synthesis. *Chem. Rev.* **2018**, *118*, 11353−11432.
(16) Montalvillo-Jimenez, L.; Santana, A. G.; Corzana, F.; Jimenez-Oses, G.; Jimenez-Barbero, J.; Gomez, A. M.; Asensio, J. L. Impact of Aromatic Stacking on Glycoside Reactivity: Balancing CH/$\pi$ and Cation/$\pi$ Interactions for the Stabilization of Glycosyl-Oxocarbenium Ions. *J. Am. Chem. Soc.* **2019**, *141*, 13372−13384.
(17) Emenike, B. U.; Bey, S. N.; Spinelle, R. A.; Jones, J. T.; Yoo, B.; Zeller, M. Cationic CH/$\pi$ interactions as a function of solvation. *Phys. Chem. Chem. Phys.* **2016**, *18*, 30940−30945.
(18) Umadevi, D.; Panigrahi, S.; Sastry, G. N. Noncovalent interaction of carbon nanostructures. *Acc. Chem. Res.* **2014**, *47*, 2574−2581.
(19) Bishop, R.; Caira, M. R.; Hayashi, N.; Higuchi, H.; Iyoda, M.; Ninomiya, K.; Nishinaga, T.; Suga, H.; Takase, M.; Tanaka, K. *Heterocyclic Supramolecules II*; Springer: Dordrecht, Heidelberg, London, New York, 2009.
(20) Tsuzuki, S.; Fujii, A. Nature and physical origin of CH/$\pi$ interaction: significant difference from conventional hydrogen bonds. *Phys. Chem. Chem. Phys.* **2008**, *10*, 2584−2594.
(21) Re, S.; Nagase, S. How is the CH/$\pi$ interaction important for mo- lecular recognition? *Chem. Commun.* **2004**, 658−658.
(22) Daze, K.; Hof, F. *Molecular Interaction and Recognition*; John Wiley & Sons, Inc.: New York, 2017.
(23) Meyer, E. A.; Castellano, R. K.; Diederich, F. Interactions with Aromatic Rings in Chemical and Biological Recognition. *Angew. Chem., Int. Ed.* **2003**, *42*, 1210−1250.
(24) Scharer, K.; Morgenthaler, M.; Paulini, R.; Obst-Sander, U.; Banner, D. W.; Schlatter, D.; Benz, J.; Stihle, M.; Diederich, F. Quantifi cation of cation−$\pi$ interactions in protein-ligand complexes: crystal-structure analysis of Factor Xa bound to a quaternary ammonium ion ligand. *Angew. Chem., Int. Ed.* **2005**, *44*, 4400−4404.
(25) Hughes, R. M.; Wiggins, K. R.; Khorasanizadeh, S.; Waters, M. L. Recognition of trimethyllysine by a chromodomain is not driven by the hydrophobic effect. *Proc. Natl. Acad. Sci. U. S. A.* **2007**, *104*, 11184−11188.
(26) Yu, Y.; Rebek, J., Jr. Reactions of Folded Molecules in Water. *Acc. Chem. Res.* **2018**, *51*, 3031−3040.
(27) Yu, Y.; Zhang, K.-D.; Petsalakis, I. D.; Theodorakopoulos, G.; Rebek, J. Asymmetric binding of symmetric guests in a water-soluble cavitand. *Supramol. Chem.* **2018**, *30*, 473−478.
(28) Rahman, F. U.; Li, Y. S.; Petsalakis, I. D.; Theodorakopoulos, G.; Rebek, J., Jr.; Yu, Y. Recognition with metallo cavitands. *Proc. Natl. Acad. Sci. U. S. A.* **2019**, *116*, 17648−17653.
(29) Rahman, F. U.; Tzeli, D.; Petsalakis, I. D.; Theodorakopoulos, G.; Ballester, P.; Rebek, J., Jr.; Yu, Y. Chalcogen Bonding and Hydrophobic Effects Force Molecules into Small Spaces. *J. Am. Chem. Soc.* **2020**, *142*, 5876−5883.
(30) Kim, Y. J.; Lek, M. T.; Schramm, M. P.S. pH influenced molecular switching with micelle bound cavitands. *Chem. Commun.* **2011**, *47*, 9636−9638.
(31) Barlow, R. B. Physiochemical Properties and Biological Activity: Thermodynamic Properties of Compounds Related to Acetylcholine Assessed From Depression of Freezing-Point and Enthalpies of Dilution. *Br. J. Pharmacol.* **1974**, *51*, 413−426.
(32) Kim, K. S.; Lee, J. Y.; Lee, S. J.; Ha, T.-K.; Kim, D. H. On Binding Forces between Aromatic Ring and Quaternary Ammonium Compound. *J. Am. Chem. Soc.* **1994**, *116*, 7399−7400.
(33) Deakyne, C. A.; Meot-Ner, M. Unconventional Ionic Hydrogen- Bonds. 2. $NH^+\cdots\pi$. Complexes of Onium Ions with Olefins and Benzene Derivatives. *J. Am. Chem. Soc.* **1985**, *107*, 474−479.
(34) Lee, J. Y.; Lee, S. J.; Choi, H. S.; Cho, S. J.; Kim, K. S.; Ha, T.-K. Ab initio study of the complexation of benzene with ammonium cations. *Chem. Phys. Lett.* **1995**, *232*, 67−71.
(35) Mecozzi, S.; West, P.; Dougherty, J. D. A. Cation-$\pi$ Interactions in Simple Aromatics: Electrostatics Provide a Predictive Tool. *J. Am. Chem. Soc.* **1996**, *118*, 2307−2308.
(36) Biros, S. M.; Ullrich, E. C.; Hof, F.; Trembleau, L.; Rebek, J. Kinetically Stable Complexes in Water: The Role of Hydration and Hydrophobicity. *J. Am. Chem. Soc.* **2004**, *126*, 2870−2876.
(37) Lascaux, A.; Leener, G.; Fusaro, L.; Topic, F.; Rissanen, K.; Luhmer, M.; Jabin, I. Selective recognition of neutral guests in an aqueous medium by a biomimetic calix[6]cryptamide receptor. *Org. Biomol. Chem.* **2016**, *14*, 738−746.
(38) Penuelas-Haro, G.; Ballester, P. Efficient hydrogen bonding recognition in water using aryl-extended calix[4]pyrrole receptors. *Chem. Sci.* **2019**, *10*, 2413−2423.
(39) Huang, G. B.; Wang, S. H.; Ke, H.; Yang, L. P.; Jiang, W. Selective Recognition of Highly Hydrophilic Molecules in Water by Endo-Functionalized Molecular Tubes. *J. Am. Chem. Soc.* **2016**, *138*, 14550−14553.
(40) Ke, C.; Destecroix, H.; Crump, M. P.; Davis, A. P. A simple and accessible synthetic lectin for glucose recognition and sensing. *Nat. Chem.* **2012**, *4*, 718−723.
(41) Tissot, A. C.; Vuilleumier, S.; Fersht, A. R. Importance of Two Buried Salt Bridges in the Stability and Folding Pathway of Barnase. *Biochemistry* **1996**, *35*, 6786−6794.
(42) Kearney, P. C.; Mizoue, L. S.; Kumpf, R. A.; Forman, J. E.; McCurdy, A.; Dougherty, D. A. Molecular Recognition in Aqueous Media. New Binding Studies Provide Further Insights into the Cation-$\pi$ Interaction and Related Phenomena. *J. Am. Chem. Soc.* **1993**, *115*, 9907−9919.


https://doi.org/10.1021/jacs.1c06510
J. Am. Chem. Soc. 2021, 143, 12397−12403